


8817

NACA TN 2421

NACA  
TN  
2421  
C.1

TECH LIBRARY KAFB, NM



0065703

# NATIONAL ADVISORY COMMITTEE FOR AERONAUTICS

TECHNICAL NOTE 2421

LOAN COPY: RETURN TO  
AFWL TECHNICAL LIBRARY  
KIRTLAND AFB, N. M.

A RAPID APPROXIMATE METHOD FOR DETERMINING VELOCITY  
DISTRIBUTION ON IMPELLER BLADES OF  
CENTRIFUGAL COMPRESSORS

By John D. Stanitz and Vasily D. Prián

Lewis Flight Propulsion Laboratory  
Cleveland, Ohio



Washington  
July 1951





0065703

1

NATIONAL ADVISORY COMMITTEE FOR AERONAUTICS

TECHNICAL NOTE 2421

A RAPID APPROXIMATE METHOD FOR DETERMINING VELOCITY DISTRIBUTION  
ON IMPELLER BLADES OF CENTRIFUGAL COMPRESSORS

By John D. Stanitz and Vasily D. Prian

2191

SUMMARY

A rapid approximate method of analysis was developed for both compressible and incompressible, nonviscous flow through radial- or mixed-flow centrifugal compressors with arbitrary hub and shroud contours and with arbitrary blade shape. The method of analysis is used to determine approximately the velocities everywhere along the blade surfaces, but no information concerning the variation in velocity across the passage between blades is given.

In eight numerical examples for two-dimensional flow, covering a fairly wide range of flow rate, impeller-tip speed, number of blades, and blade curvature, the velocity distribution along the blade surfaces was obtained by the approximate method of analysis and compared with the velocities obtained by relaxation methods. In all cases the agreement between the approximate solutions and the relaxation solutions was satisfactory except at the impeller tip where the velocities obtained by the approximate method did not, in general, become equal on both surfaces of the blade as required by the Joukowski condition.

INTRODUCTION

In impellers of centrifugal compressors, part of the viscous losses and the phenomena of surge and choke are related to the velocity distribution on the blade surfaces. Viscous losses in impellers are associated with the boundary layer along the flow surfaces. The growth of this boundary layer depends on the velocity variation along the flow surfaces just outside of the boundary layer. In particular, if the velocity decelerates rapidly along the blade surfaces, the boundary layer may separate causing large mixing losses. Also, if the velocity at any point along the blade surface is sufficiently greater than the local speed of sound, shock losses will result. The choke phenomenon occurs when the average velocity between blades is sonic. This average sonic velocity is characterized by local supersonic velocities along portions of the suction surface of the blade. One possible cause of

surge in centrifugal impellers is the formation of relative eddies on the pressure surface of the blade (reference 1). These eddies are characterized by negative velocities, opposed to the general flow direction, along portions of the pressure surface. In order to analyze the performance of centrifugal impellers it is therefore necessary to determine the velocity distribution on impeller blades.

Several methods of analysis that can be used to determine the variation in velocity along blades with finite spacing have been developed for two-dimensional incompressible flow (references 2 to 5, for example) and compressible flow (references 1 and 6). All these methods require considerable labor and therefore are not convenient tools for analyzing the performance of an arbitrary impeller design.

In this report a rapid approximate method developed at the NACA Lewis laboratory is presented for both compressible and incompressible, nonviscous, two-dimensional flow between blades with finite spacing in radial- or mixed-flow centrifugal compressors with arbitrary hub and shroud contours and with arbitrary blade shape. The method of analysis can be used in connection with an axial-symmetry solution to determine the velocities everywhere along the blade surfaces, but no information concerning the variation in velocity across the passage between blades is given.

Other approximate methods that are less rapid than the proposed method for computing the velocity distribution on blade surfaces in impellers of centrifugal pumps and compressors are given in references 6 to 9. In the sections SIMPLIFIED ANALYSIS of references 6 and 7 approximate methods are developed for computing the theoretical distribution of velocity across the passage along normals to the blade surfaces. The methods are limited to straight or logarithmic-spiral blade shapes on radial or conic surfaces of revolution and do not apply, because of assumptions, in regions near the impeller tip and the impeller inlet. In reference 8 methods are developed for computing the distribution of velocity across the passage between blades in the circumferential direction for incompressible flow with arbitrary blade shapes and with arbitrary hub and shroud contours. The methods do not apply, because of assumptions, in regions near the impeller tip and the impeller inlet. In reference 9 an approximate method is developed for computing the theoretical velocity distribution everywhere within the impeller. In this method the corrections required for compressibility and for blade unloading at the tip are somewhat more complicated than those presented herein.

#### THEORY OF METHOD

The method of analysis presented in this section determines the velocity distribution along the profiles of blade elements on surfaces of revolution.

1612

### Preliminary Considerations

2191 Assumed nature of flow. - In this section certain preliminary assumptions are made concerning the three-dimensional flow of an ideal compressible fluid through an arbitrary impeller passage between blades such as shown in figure 1. In general, the fluid is free to follow whatever path the pressure and inertia forces require of it. If, however, it is assumed that the number of blades in the impeller approaches infinity, the space between blades approaches zero and the path of the fluid is restricted to the curved, mean surface of the blade. (The blades become very thin so that the two surfaces of each blade approach a mean surface.) Under this assumption of axial symmetry the fluid motion is reduced from a general three-dimensional motion to a two-dimensional motion on the curved, mean blade surface. The streamlines of this two-dimensional motion can be projected on the meridional (axial-radial) plane, as shown in figure 2. Ruden (reference 10) has shown that, provided that the blades are not too widely spaced, axial-symmetry solutions give a good picture of the mean flow between blades.

For finite blade spacing, flow conditions vary between blades in the circumferential direction about the axis of the impeller. In order to investigate this blade-to-blade variation, it is assumed that the motion of any fluid particle bounded by adjacent streamlines in the meridional plane (fig. 2) is restricted to the annulus generated by rotating these adjacent streamlines about the axis of the impeller. If the adjacent streamlines are sufficiently close together, flow conditions in the annulus can be considered uniform normal to a mean surface of revolution in the annulus. Thus the fluid motion is reduced to two-dimensional flow on the mean surface of revolution (fig. 3) generated by rotating the center line between the adjacent streamlines in the meridional plane (fig. 2) about the axis of the impeller.

Blade-to-blade solutions of this type may be obtained for every mean surface of revolution generated by the center lines between adjacent streamlines in the meridional plane. Therefore, flow conditions can be determined throughout the passage between blades. The resulting quasi three-dimensional solution is obtained by the combination of two types of two-dimensional solution, axial-symmetry solutions in the meridional plane and blade-to-blade solutions on surfaces of revolution. Such a combination of solutions prohibits the possibility of a corkscrew path, which the fluid might follow in an exact three-dimensional solution, but it can be expected to give a better picture of the flow than does any two-dimensional solution alone.

The method of analysis just described is accomplished in two phases, axial-symmetry solution and blade-to-blade solutions. Only the second phase, blade-to-blade solutions, will be considered in this

report. The shape and the distribution of meridional streamlines in the axial-radial plane are assumed to be known from an axial-symmetry solution (reference 11, for example). Thus, for a blade-to-blade solution in the annulus generated about the axis of the impeller by any two adjacent meridional streamlines (fig. 2), the shape of the mean surface of revolution (fig. 3) is known from the shape of the center line between the adjacent meridional streamlines, and the variation in height of an elementary fluid particle (fig. 2) as it moves along the mean surface of revolution from the impeller inlet to the impeller tip is known from the variation in spacing of the adjacent meridional streamlines.

Coordinates. - The cylindrical coordinates  $R$ ,  $\theta$ , and  $Z$  are shown in figure 3. (All symbols are defined in the appendix.) These coordinates are dimensionless, the linear coordinates  $R$  and  $Z$  having been divided by the impeller-tip radius  $r_T$ . The coordinate system is oriented with the  $Z$ -axis along the axis of the impeller. The coordinates are fixed relative to the impeller, which rotates with the angular velocity  $\omega$  in the positive direction (right-hand rule) about the  $Z$ -axis, as shown in figure 3.

An infinitesimal distance  $dS$  in the direction of flow (that is, coinciding with the velocity vector) has components  $dR$ ,  $Rd\theta$ , and  $dZ$  (fig. 3). The projection of  $dS$  on the meridional plane is given by  $dM$  in figure 3. The infinitesimal distances  $dS$  and  $dM$  help to define two angles  $\alpha$  and  $\beta$  where, from figure 3,

$$dR = dM \sin \alpha \tag{1a}$$

$$dZ = dM \cos \alpha \tag{1b}$$

and

$$dM = dS \cos \beta \tag{2a}$$

$$Rd\theta = dS \sin \beta \tag{2b}$$

The angle  $\alpha$  (fig. 3) is determined by tangents to the center line, between adjacent meridional streamlines, that generates the surface of revolution. The angle  $\beta$  (fig. 3) is the flow direction on the surface of revolution measured from a meridional line. From equation (2a)

$$-\frac{\pi}{2} \leq \beta \leq \frac{\pi}{2}$$

because  $dS$  and  $dM$  are always positive and finite. From equations (1a) and (1b),

$$0 \leq \alpha \leq \frac{\pi}{2}$$

2191

because for impellers of centrifugal compressors  $dR$  and  $dZ$  will be considered positive (or zero).

Fluid strip. - A fluid strip of infinitesimal width  $dM$  lies on the surface of revolution and extends across the passage between blades along a line of constant  $R$ . A developed view of the fluid strip is shown in figure 4. The fluid strip has dimensions  $dM$  and  $R\Delta\theta$  where the angular width of passage between blades  $\Delta\theta$  is defined by

$$\Delta\theta = \theta_t - \theta_d \tag{3}$$

in which the subscripts  $d$  and  $t$  refer to the driving and trailing faces of the blades, respectively (left and right walls of the channel between blades in fig. 4). The height ratio  $H$  of the fluid strip is defined as the ratio of the incremental height  $\Delta h$  (fig. 2) of the fluid strip at radius  $R$  to the incremental height  $(\Delta h)_T$  of the fluid strip at  $R = 1.0$ . This height ratio is completely determined along a mean surface of revolution by the spacing between the adjacent streamlines in the meridional plane (fig. 2).

Velocity components. - The relative velocity  $Q$  on a surface of revolution has components  $Q_M$  and  $Q_\theta$  in the  $dM$  and  $d\theta$  directions, respectively, (fig. 3). These velocities are dimensionless, having been divided by the absolute stagnation speed of sound  $c_o$  upstream of impeller, where

$$c_o^2 = \gamma gRT_o \tag{4}$$

in which  $R$  is the gas constant,  $\gamma$  is the ratio of specific heats,  $T$  is the static (stream) temperature and where the subscript  $o$  refers to stagnation conditions upstream of the impeller. The tip speed of the impeller is likewise dimensionless and equal to the impeller-tip Mach number  $M_T$ , which is defined by

$$M_T = \frac{\omega r_T}{c_o} \tag{5}$$

Thus, the tangential velocity of the impeller at any radius  $R$  is equal to  $RM_T$  and the absolute tangential velocity of the fluid is equal to  $(RM_T + Q_\theta)$ . From figure 3

$$Q_M = Q \cos \beta \tag{6}$$

and

$$Q_\theta = Q \sin \beta \tag{7}$$

2191

Thermodynamic relations. - From the general energy equation and from the isentropic relation between temperature and density, the density ratio  $\rho/\rho_0$  is related to the relative velocity  $Q$  by

$$\frac{\rho}{\rho_0} = \left\{ 1 + \frac{\gamma-1}{2} \left[ (RM_T)^2 - Q^2 - 2M_T \lambda U \right] \right\}^{\frac{1}{\gamma-1}} \quad (8)$$

where the subscript  $U$  refers to conditions upstream of the impeller and where  $\lambda$  is the whirl ratio (absolute moment of momentum divided by  $r_T c_0$ ) given by

$$\lambda = R(RM_T + Q\theta) \quad (9)$$

#### Development of Method

Assumptions. - Before outlining the method of analysis it is convenient to discuss the major assumptions. Consider the fluid strip in figure 4. Along the infinitesimal distances bounding the fluid strip at the driving and trailing blade surfaces, the velocities may be considered constant and equal to  $Q_d$  and  $Q_t$ , respectively, and the flow directions may be considered constant and equal to  $\beta_d$  and  $\beta_t$ . Along the lines of constant  $R$  bounding the fluid strip in figure 4, the velocity varies in some unknown manner from  $Q_d$  to  $Q_t$  and the flow direction varies from  $\beta_d$  to  $\beta_t$ . In this report it is assumed that the average values of  $Q$  and  $\beta$  along lines of constant  $R$  may be used to satisfy the conditions of continuity and absolute irrotational motion. The average value of  $Q$  is assumed to be given by

$$Q_{av} = \frac{Q_d + Q_t}{2} \quad (10)$$

and, for  $R \leq R_x$ , the average value of  $\beta$  is assumed to be given by

$$\beta_{av} = \frac{\beta_d + \beta_t}{2} \quad (11)$$

Also, for  $R_x \leq R \leq 1.0$ ,

$$\sin \beta_{av} = A + BR + CR^2 \quad (12)$$

2191

where A, B, and C are coefficients to be determined and where  $R_x$  is the largest radius at which the fluid is considered to be perfectly guided by the blades; that is, the radius at which the simplified analyses given in references 6 and 7 break down. From figure 10 of reference 7 the value of  $R_x$  for  $\Delta\theta$  equal to  $\pi/10$  and  $\sin \alpha$  equal to 1.0 is about 0.8. For other values of  $\Delta\theta$  and  $\sin \alpha$ , the value of  $R_x$  can be estimated from

$$\frac{\ln R_x}{(\Delta\theta) \sin \alpha} = \frac{\ln 0.8}{\pi/10} = - 0.71 \quad (13)$$

where  $\alpha$  is the average value over the interval  $R_x \leq R \leq 1.0$ . Equation (13) is based upon an extension of the work in reference 1 where for impellers with straight blades it is shown that the flow conditions in one impeller can be correlated with the flow conditions in another impeller at the same value of  $\frac{\ln R}{(\Delta\theta) \sin \alpha}$ . In reference 1, the impeller-tip Mach number and the compressor flow rate were found to have a negligible effect on the value of  $R_x$ .

Outline of theory. - Fluid strips such as shown in figure 4 exist at all radii along the surface of revolution. From the assumptions of this analysis there are three unknowns ( $Q_d$ ,  $Q_t$ , and  $Q_{av}$ ) for each fluid strip. These unknowns can be determined by the simultaneous solution of equation (10) and the equations of continuity and zero absolute circulation for flow across the fluid strip. Equations for the distribution of velocity along the blade profile on a surface of revolution will be developed in this report.

Zero absolute circulation. - In the absence of entropy gradients, which result from shock, viscous dissipation, heat transfer, and so forth, the absolute circulation around the fluid strip in figure 4 is zero so that

$$(Q + RM_T \sin \beta)_d \frac{dM}{\cos \beta_d} - (Q + RM_T \sin \beta)_t \frac{dM}{\cos \beta_t} + \frac{d}{dM} \left[ (RM_T + Q_\theta)_{av} R \Delta\theta \right] dM = 0 \quad (14)$$

where  $(RM_T + Q_\theta)_{av}$  is the average absolute tangential velocity and where from trigonometric considerations of the velocity triangles (fig. 5)  $Q + RM_T \sin \beta$  is the absolute velocity component along the blade surface. From equations (7) and (14) and from the assumptions that  $Q$  and  $\beta$  equal  $Q_{av}$  and  $\beta_{av}$ , respectively, in the passage between blades,

2191



$$\frac{Q_d}{\cos \beta_d} - \frac{Q_t}{\cos \beta_t} + RM_T (\tan \beta_d - \tan \beta_t) + \frac{d}{dM} \left[ (RM_T + Q_{av} \sin \beta_{av}) R \Delta \theta \right] = 0 \quad (15)$$

Finally, from equations (10) and (15)

$$Q_t = \frac{\cos \beta_d \cos \beta_t}{\cos \beta_t + \cos \beta_d} \left\{ \frac{2 Q_{av}}{\cos \beta_d} + RM_T (\tan \beta_d - \tan \beta_t) + \frac{d}{dM} \left[ (RM_T + Q_{av} \sin \beta_{av}) R(\Delta \theta) \right] \right\} \quad (16)$$

and from equation (11)

$$Q_d = 2Q_{av} - Q_t \quad (17)$$

If  $Q_{av}$  and  $\beta_{av}$  are known,  $Q_d$  and  $Q_t$  can be determined from equations (16) and (17).

Average velocity  $Q_{av}$ . - From continuity considerations of the flow across the fluid strip in figure 4,

$$\Delta w = \left( \rho_o \frac{\rho_{av}}{\rho_o} \right) (c_o Q_{av}) \cos \beta_{av} \left[ (\Delta h)_T H \right] (r_T R) \Delta \theta$$

from which

$$Q_{av} = \frac{\varphi}{\frac{\rho_{av}}{\rho_o} \cos \beta_{av} HR \frac{\Delta \theta}{(\Delta \theta)_T}} \quad (18)$$

where the flow coefficient  $\varphi$  is defined by

$$\varphi = \frac{1}{\rho_o c_o} \frac{\Delta w}{(\Delta a)_T} \quad (19)$$

in which  $\Delta w$  is the incremental flow rate through the passage between two blades on the surface of revolution and  $(\Delta a)_T$  is the incremental flow area (between two blades) normal to the direction of  $Q_M$  at the impeller tip

$$(\Delta a)_T = r_T (\Delta \theta)_T (\Delta h)_T \quad (19a)$$

11/18

The flow rate per unit flow area at the impeller tip  $\Delta w/(\Delta a)_T$  is known so that the flow coefficient  $\phi$  can be determined by equation (19). The density ratio  $\rho_{av}/\rho_0$  is given by equation (8) with  $Q$  equal to  $Q_{av}$

$$\frac{\rho_{av}}{\rho_0} = \left\{ 1 + \frac{\gamma-1}{2} \left[ (RM_T)^2 - Q_{av}^2 - 2\lambda_{JT} M_T \right] \right\}^{\frac{1}{\gamma-1}} \quad (20)$$

2191

Therefore, the velocity  $Q_{av}$  can be determined by the simultaneous solution of equations (18) and (20) provided that the average flow direction  $\beta_{av}$  is known.

Average flow direction. - In the passage between blades the average flow direction is assumed equal to the average blade direction (equation (11)) except near the blade tip ( $R_x \leq R \leq 1.0$ ) where  $\sin \beta_{av}$  is given by equation (12). The exact variation in  $\beta_{av}$  with  $R$  in the interval  $R_x \leq R \leq 1.0$  could be represented by an infinite series. However, because the variation in  $\sin \beta_{av}$  with  $R$  will not, in general, contain an inflection point, a parabolic variation in  $\sin \beta_{av}$  with  $R$  has been assumed and only the first three terms of the infinite series retained. The constants  $A$ ,  $B$ , and  $C$  in equation (12) are determined from:

$$(1) \quad (\sin \beta_{av})_x = A + BR_x + CR_x^2$$

$$(2) \quad \left( \frac{d \sin \beta_{av}}{dR} \right)_x = B + 2CR_x$$

and

$$(3) \quad (\sin \beta_{av})_T = A + B + C$$

so that

$$\left. \begin{aligned} A &= (\sin \beta_{av})_T - B - C \\ B &= \left( \frac{d \sin \beta_{av}}{dR} \right)_x - 2R_x C \\ C &= \frac{1}{(1-R_x)^2} \left[ (\sin \beta_{av})_T - (\sin \beta_{av})_x - (1-R_x) \left( \frac{d \sin \beta_{av}}{dR} \right)_x \right] \end{aligned} \right\} (21)$$

where  $(\sin \beta_{av})_x$  and  $\left(\frac{d \sin \beta_{av}}{dR}\right)_x$  are known from the blade geometry at  $R_x$ , and where  $(\sin \beta_{av})_T$  is determined from the slip factor  $\mu$ , which is defined by (reference 6)

$$\mu = 1 + \frac{(Q_{av} \sin \beta_{av})_T}{M_T}$$

so that

$$(\sin \beta_{av})_T = \frac{M_T (\mu - 1)}{(Q_{av})_T} \quad (22)$$

The slip factor  $\mu$  is assumed to be known, or can be estimated, as a result of the work presented in references 1 and 7, for example. (Further discussion on  $R_x$  and the slip factor  $\mu$  is given later in this report.) The velocity  $(Q_{av})_T$  in equation (22) is obtained from equations (18) and (20) with  $R$  and  $H$  equal to 1.0 and with  $(\cos \beta_{av})_T$  replaced by  $\sqrt{1 - (\sin \beta_{av})_T^2}$  where  $(\sin \beta_{av})_T$  is given by equation (22):

$$(Q_{av})_T = \frac{\varphi}{\left\{ 1 + \frac{\gamma - 1}{2} \left[ (M_T)^2 - (Q_{av})_T^2 - 2\lambda U M_T \right] \right\}^{\frac{1}{\gamma - 1}} \sqrt{1 - \left[ \frac{M_T (\mu - 1)}{(Q_{av})_T} \right]^2}} \quad (23)$$

Equation (23) is solved for  $(Q_{av})_T$  by trial and error. Therefore,  $\beta_{av}$  is determined as a function of  $R$  (or  $M$ ) by equations (11), (12), and (21). The velocities  $Q_d$ ,  $Q_t$ , and  $Q_{av}$  are determined as functions of  $M$  (or  $R$ ) from equations (16), (17), and (18). (The last term of equation (16) is determined from the slope of  $(RM_T + Q_{av} \sin \beta_{av}) R (\Delta\theta)$  plotted against  $M$ .)

#### APPLICATION OF METHOD

The following outline of the numerical procedure is given for the general case of a mixed-flow impeller with arbitrary hub and shroud contours in the meridional plane (fig. 2) and arbitrary blade shape (curvature and thickness distribution) on surfaces of revolution. It is assumed that the surfaces of revolution are known, that is have been generated by the center lines between adjacent meridional streamlines

2191

obtained from an axial symmetry solution (reference 11, for example). The following outline of the numerical procedure refers to any one of these surfaces of revolution.

Specified conditions. - The following quantities are specified:

- (1) Flow coefficient  $\phi$  (defined by equation (19) in which  $\rho_o$ ,  $c_o$ ,  $\Delta w$ , and  $(\Delta a)_{\Gamma}$  are known quantities)
- (2) Impeller-tip Mach number  $M_{\Gamma}$  (defined by equation (5))
- (3) Whirl ratio  $\lambda_{\Gamma}$  upstream of impeller (defined by equation (9))
- (4) Ratio of specific heats  $\gamma$
- (5) From the shape of the center line between adjacent meridional streamlines that generate the surface of revolution,

$$R = R(M)$$

and

$$\alpha = \alpha(M)$$

where the distance  $M$  along a meridional line on the surface of revolution is arbitrarily equal to zero at the impeller tip and decreases toward the impeller inlet

- (6) From the spacing of the adjacent meridional streamlines,

$$H = H(M)$$

Variation in  $\sin \beta_{av}$ . - The variation in  $\sin \beta_{av}$  with  $R$  near the impeller tip ( $R_x \leq R \leq 1.0$ ) is determined as follows:

- (1) Compute the value of  $R_x$  by equation (13). If  $\sin \alpha$  varies in the region  $R_x \leq R \leq 1.0$ , as it generally does, the average value of  $\alpha$  in this region is used in equation (13), and because the average value of  $\alpha$  varies with the value of  $R_x$ , equation (13) must be solved by trial and error. However, because the value of  $\alpha$  does not generally vary greatly in the region  $R_x \leq R \leq 1.0$ , a satisfactory value of  $R_x$  could be obtained from equation (13) using the average value of  $\alpha$  obtained from an initially assumed value of  $R_x$ . Also, equation (13) was developed from information (references 1 and 7) relating to blades that are not designed to unload at the tip. If the blades being considered were designed to unload at the tip, the direction of the mean flow path near the impeller tip would deviate less from the mean blade direction and the

2191

value of  $R_x$  would be somewhat greater than that given by equation (13). The value of  $R_x$  is not especially critical and in these cases, with sufficient experience, it can probably be estimated accurately enough from the radius at which an assumed path of the mean streamline (sketched by experience) deviates appreciably from the mean direction of the blade profile on the surface of revolution.

- (2) Estimate the value of  $\mu$ , or obtain values from references 1 and 7. The values of  $\mu$  given in references 1 and 7 were obtained for blades that are not designed to unload at the tip. If the blades being considered were designed to unload at the tip, the direction of the mean flow path at the impeller tip would deviate less from the mean blade direction at the tip and the value of  $\mu$  would be somewhat greater than that indicated in references 1 and 7; that is,  $(\beta_{av})_T$  would be more nearly equal to  $\frac{1}{2}(\beta_d + \beta_t)_T$ . The value of  $\mu$ , like the value of  $R_x$ , is not especially critical and in these cases it can probably be estimated accurately enough from the assumed shape of a mean streamline (sketched from experience) between blade-element profiles on the surface of revolution.
- (3) Compute  $(Q_{av})_T$  from equation (23) by trial and error.
- (4) Compute  $(\sin \beta_{av})_T$  from equation (22).
- (5) Compute coefficients A, B, and C from equations (21).
- (6) Compute  $\sin \beta_{av}$  over the interval  $R_x \leq R \leq 1.0$  by equation (12).

The variation in  $\beta_{av}$  for  $R$  less than  $R_x$  is given by equation (11). This equation is assumed to be valid downstream to the impeller inlet. If the angle of attack at the impeller inlet is zero, the assumption is probably good. If the angle of attack is small, the error involved is probably small and could be partly corrected by estimating the path of the mean streamline between blades in this region. For large angles of attack, the stagnation point on the blade surface may exist well inside the impeller passage and the ideal flow is reversed along the blade surface downstream of this point. Under these conditions, the method of analysis does not apply near the impeller inlet but because of the high blade solidity it does apply elsewhere in the impeller.

2191

2191

Average velocity  $Q_{av}$ . - The average velocity  $Q_{av}$  at each value of  $M$  (or  $R$ ) is determined by equation (18) in which  $\rho_{av}/\rho_0$  is given by equation (20). Because  $\rho_{av}/\rho_0$  also contains  $Q_{av}$ , the simultaneous solution of equations (18) and (20) must be by trial and error. A suggested procedure is first to compute  $\rho_{av}/\rho_0$  assuming that  $Q_{av}$  in equation (20) is zero. This value of  $\rho_{av}/\rho_0$  is then used to compute  $Q_{av}$  by equation (18). The process is repeated each time using the new value of  $Q_{av}$  to compute  $\rho_{av}/\rho_0$  until the value of  $Q_{av}$  converges.

Velocities on blade surfaces,  $Q_d$  and  $Q_t$ . - The velocities on the blade surfaces at each value of  $M$  (or  $R$ ) are determined by equations (16) and (17). The last term in equation (16) is obtained from the slope of  $(RM_T + Q_{av} \sin \beta_{av}) R (\Delta\theta)$  plotted against  $M$ .

Finally, the static (stream) pressure  $p$  corresponding to the relative velocity  $Q$  at any radius  $R$  is given by

$$\frac{p}{p_0} = \left(\frac{\rho}{\rho_0}\right)^\gamma = \left\{ 1 + \frac{\gamma-1}{2} \left[ (RM_T)^2 - Q^2 - 2M_T \lambda U \right] \right\}^{\frac{\gamma}{\gamma-1}} \quad (24)$$

#### NUMERICAL EXAMPLES

The approximate analysis method developed in this report is applied to eight examples for which relaxation solutions of the exact differential equation for two-dimensional compressible flow in impellers of centrifugal compressors are given in references 1 and 7. Although these examples are for radial- or conic-flow surfaces and not for arbitrary surfaces of revolution, they cover a fairly wide range of design and operating variables so that a comparison of the velocities (on the blade surfaces) obtained by the relaxation solutions and by the approximate analysis method should serve as a check on the validity of the approximate method.

Types of impeller. - The eight numerical examples are for two-dimensional radial-flow impellers for which  $\alpha$  is equal to  $90^\circ$  and the surfaces of revolution are flat planes normal to the axes of the impellers. The impellers (fig. 6) contain a finite number of thin straight ( $\beta_d = \beta_t = 0$ ) or logarithmic-spiral ( $\beta_d = \beta_t = \text{constant}$ ) blades, and the flow area normal to the direction of  $Q_M$  is constant so that  $HR$  equals 1.0. Only the critical flow region toward the tip of the impeller was investigated ( $0.70 \leq R \leq 1.0$ ). The diffuser vanes (if any) and the inducer vanes were assumed to be far enough removed not to affect the flow in this region.

Design and operating variables. - The following design and operating variables were specified for the eight examples:

Example	$\phi$	$M_T$	$\Delta\theta$	$\tan \beta$	Fluid	$\mu$
(a)	0.5	1.5	$2\pi/30$	0	Compressible	0.934
(b)	.7	1.5	$2\pi/30$	0	Compressible	.937
(c)	.9	1.5	$2\pi/30$	0	Compressible	.938
(d)	.5	2.0	$2\pi/30$	0	Compressible	.935
(e)	.5	1.5	$2\pi/20$	0	Compressible	.899
(f)	.5	1.5	$2\pi/20$	-0.5	Compressible	.834
(g)	.5	1.5	$2\pi/20$	-1.0	Compressible	.768
(h)	.5	1.5	$2\pi/20$	0	Incompressible	.892

The whirl ratio upstream of the impeller  $\lambda_U$  was zero and for the compressible fluid the ratio of specific heats  $\gamma$  was 1.4. The value of the slip factor  $\mu$  given in the table was obtained from the relaxation solutions and was also used to compute  $(\sin \beta_{av})_T$  in equation (22). For the incompressible example, the speed of sound  $c_0$  contained in the definitions of  $Q$ ,  $\phi$ , and  $M_T$  is a fictitious quantity (constant) considered equal to the upstream stagnation speed of sound of the compressible-flow examples with which the incompressible-flow example is compared.

Results. - The results of the comparison between the relaxation solutions and the approximate method of analysis are shown in figure 7 for the eight examples. The velocities  $Q_d$  and  $Q_t$  are plotted against  $R$  for the relaxation solutions and for the approximate solutions. The average velocity  $Q_{av}$  used in the approximate method of analysis to obtain  $Q_d$  and  $Q_t$  is also plotted.

The effect of increasing the flow rate (flow coefficient) on the agreement between the relaxation solution and the approximate solution is shown in figures 7(a) to 7(c). The agreement appears equally good for all flow rates. In view of the relative simplicity of the approximate method of analysis, the agreement is considered entirely satisfactory everywhere except in the immediate vicinity of the impeller tip where the results of the approximate method of analysis do not follow the rapid unloading of the blades. This rapid unloading is characteristic of blades that are not designed to unload at the tip. If the blades were designed to unload, the agreement between relaxation solutions and approximate solutions should be better. In any event the disagreement is serious only over the last 2 percent of impeller-tip radius. The failure to unload at the impeller tip will be observed in most of the remaining solutions.

2191

The following figure comparisons indicate: figures 7(a) and 7(d), the effect of increasing impeller-tip Mach number; figures 7(a) and 7(e), the effect of increasing angular width of passage between blades ( $\Delta\theta$ ); figures 7(e), 7(f), and 7(g), the effect of larger negative blade angles  $\beta$ ; and figures 7(e) and 7(h), the effect of compressibility. In figure 7(h), the peculiar humps in the velocity distribution obtained by the approximate method of analysis indicates that for incompressible flow the blades start to unload at a lower value for  $R_x$  than that given by equation (13).

In view of the relative simplicity of this approximate, but rapid, method of analysis, the agreement between the relaxation solutions and the approximate solutions is considered good in all cases investigated; that is, over fairly wide ranges of flow rate, impeller-tip speed, blade curvature, and number of blades.

#### SUMMARY OF RESULTS

A rapid approximate method of analysis was developed for determining the velocity distribution on impeller blades of centrifugal compressors. In eight numerical examples the velocities obtained by the approximate method of analysis were compared with the more nearly correct values obtained by relaxation methods. In all cases, that is, over a fairly wide range of flow rate, impeller-tip speed, blade curvature, and number of blades, the agreement between velocities obtained by the approximate method of analysis and by relaxation methods was considered good.

Lewis Flight Propulsion Laboratory,  
National Advisory Committee for Aeronautics,  
Cleveland, Ohio, April 27, 1951.

2191



APPENDIX - SYMBOLS

The following symbols are used in this report:

- A,B,C coefficients defined by equation (21)
- $c_0$  stagnation speed of sound upstream of impeller, equation (4)
- $g$  acceleration due to gravity
- H height ratio of fluid strip normal to surface of revolution,  
 $\Delta h / (\Delta h)_T$
- M distance along meridional line on surface of revolution  
 (dimensionless, expressed as ratio of impeller tip radius  $r_T$ )  
 (fig. 3)
- $M_T$  impeller tip Mach number, equation (5)
- $p$  static (stream) pressure
- Q relative velocity on surface of revolution (dimensionless,  
 expressed in units of the stagnation speed of sound upstream  
 of impeller  $c_0$ ) (fig. 3)
- R cylindrical coordinate (dimensionless, expressed as ratio of  
 impeller-tip radius  $r_T$ ) (fig. 3)
- $r_T$  impeller-tip radius
- S distance along streamline on surface of revolution (dimension-  
 less, expressed as ratio of impeller-tip radius  $r_T$ ) (fig. 3)
- T static (stream) temperature
- Z cylindrical coordinate (dimensionless, expressed as ratio of  
 impeller-tip radius  $r_T$ ) (fig. 3)
- $\alpha$  slope of surface of revolution in direction of  $Q_M$ , equa-  
 tions (1a) and (1b) (fig. 3)
- $\beta$  flow direction on surface of revolution, equations (2a) and (2b),  
 (fig. 3)
- $\gamma$  ratio of specific heats
- $(\Delta a)_T$  incremental flow area between two blades and normal to the  
 direction of  $Q_M$  at impeller tip, equation (19a)

2191

1612  
2191

- $\Delta h$  incremental height of fluid strip on surface of revolution
- $\Delta w$  incremental flow rate between two blades on surface of revolution
- $\Delta\theta$  angular width of passage between blades, radians unless otherwise specified, equation (3)
- $\theta$  cylindrical coordinate, radians unless otherwise specified, (positive about Z-axis according to right-hand rule) (fig. 3)
- $\lambda$  whirl ratio, equation (9)
- $\mu$  slip factor, equation (22)
- $\rho$  static (stream) weight density of fluid
- $\varphi$  flow coefficient, equation (19)
- $\omega$  angular velocity of impeller (in direction of positive  $\theta$ )

Subscripts:

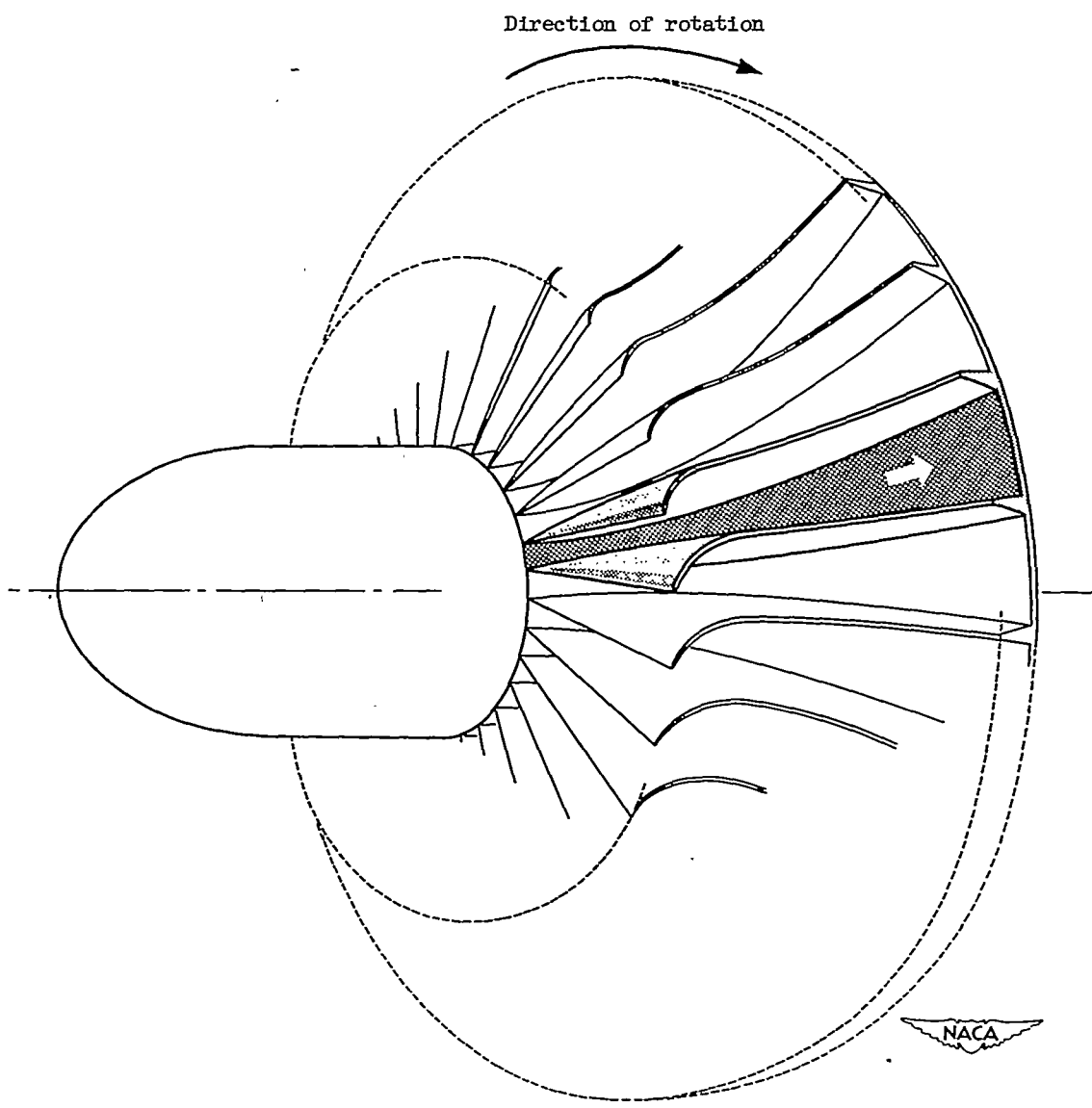
- abs component of absolute velocity along blade surface
- av average
- d driving face of blade (blade surface in direction of rotation) (fig. 4)
- M component along meridional line on surface of revolution
- o absolute stagnation condition upstream of impeller
- R, $\theta$ ,Z components in positive R-,  $\theta$ -, Z-directions, respectively
- T impeller tip
- t trailing face of blade (blade surface opposed to direction of rotation) (fig. 4)
- U upstream of impeller
- x position along meridional line on surface of revolution at which the assumption of perfect guiding of fluid by blades is considered to break down

REFERENCES

1. Stanitz, John D., and Ellis, Gaylord O.: Two-Dimensional Compressible Flow in Centrifugal Compressors with Straight Blades. NACA Rep. 954, 1950.
2. Concordia, C., and Garter, G. K.: D-C Network-Analyzer Determination of Fluid-Flow Pattern in a Centrifugal Impeller. Jour. Appl. Mech., vol. 14, no. 2, June 1947, pp. A113-A118.
3. Sørensen, E.: Potential Flow Through Centrifugal Pumps and Turbines. NACA TM 973, 1941.
4. Spannhake, W.: Anwendung der konformen Abbildung auf die Berechnung von Strömungen in Kreiselpumpen. Z.f.a.M.M., Bd. 5, Heft 6, Dez. 1925, S. 481-484.
5. Busemann, A.: Das Förderhöhenverhältnis radialer Kreiselpumpen mit logarithmisch-spiraligen Schaufeln. Z.f.a.M.M., Bd. 8, Heft 5, October 1928, P. 372-384.
6. Stanitz, John D.: Two-Dimensional Compressible Flow in Turbomachines with Conic Flow Surfaces. NACA TN 1744, 1948.
7. Ellis, Gaylord O., and Stanitz, John D.: Two-Dimensional Compressible Flow in Centrifugal Compressors with Logarithmic-Spiral Blades. NACA TN 2255, 1951.
8. Spannhake, Wilhelm: Centrifugal Pumps, Turbines and Propellers. The Technology Press (Cambridge), 1934.
- √ 9. Sheets, H. E.: The Flow Through Centrifugal Compressors and Pumps. ASME Trans., vol. 72, no. 7, Oct. 1950, pp. 1009-1015.
10. Ruden, P.: Investigation of Single Stage Axial Fans. NACA TM 1062, 1944.
11. Hamrick, Joseph T., Ginsburg, Ambrose, and Osborn, Walter M.: Method of Analysis for Compressible Flow through Mixed-Flow Centrifugal Impellers of Arbitrary Design. NACA TN 2165, 1950.

2191

T6T2



2017

Figure 1. - Passage between blades in impeller of typical centrifugal compressor.

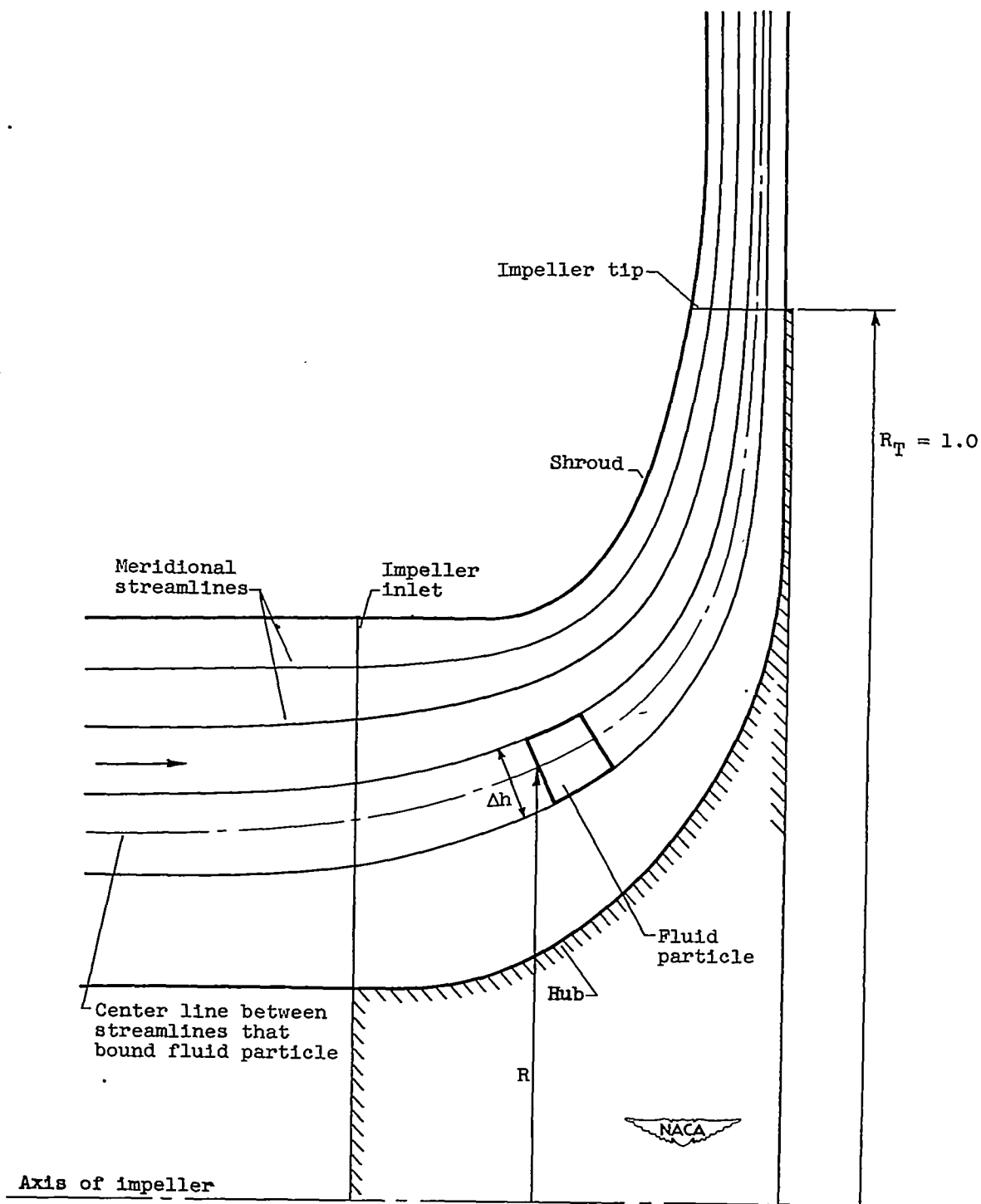


Figure 2. - Streamlines in meridional plane for axial-symmetry solution of flow through impeller of figure 1.

2191

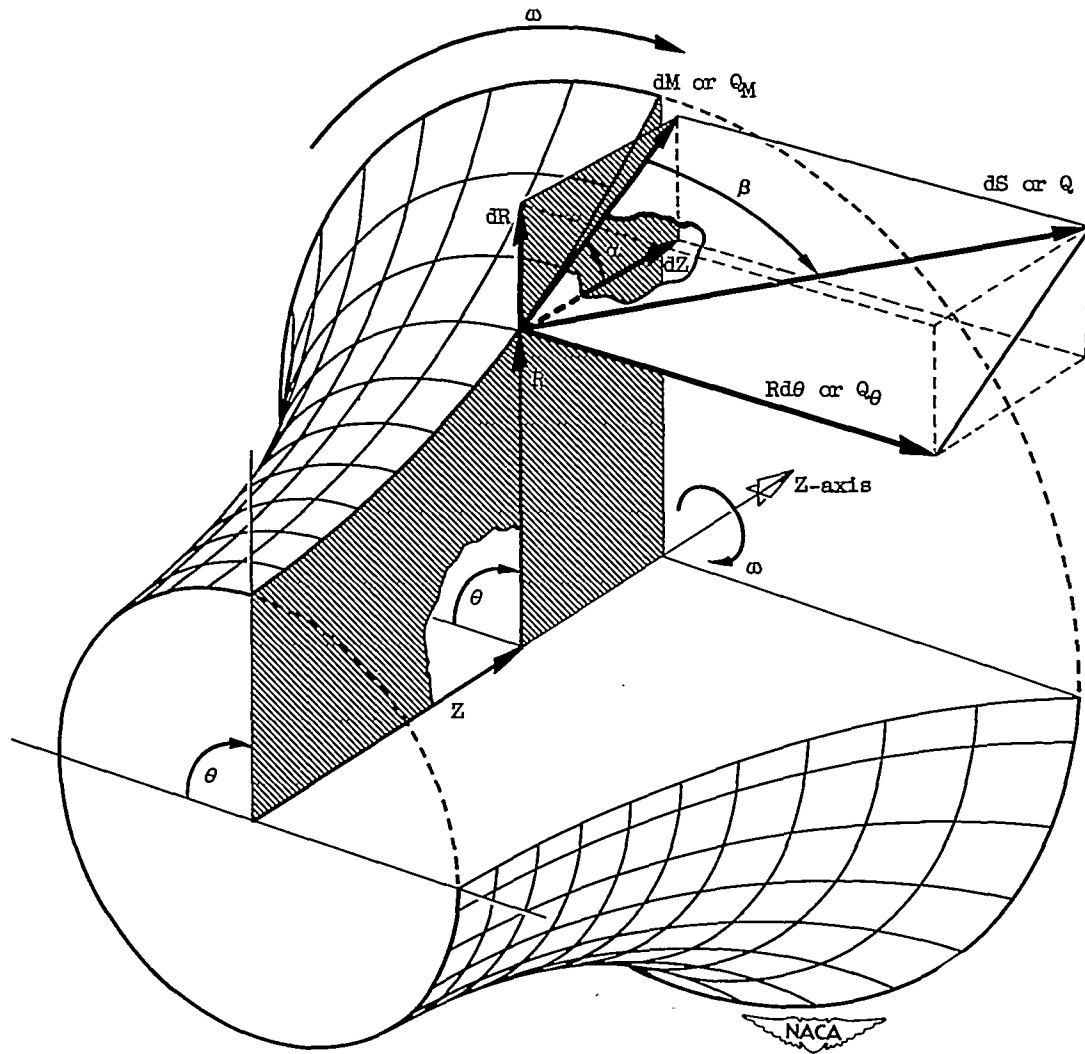


Figure 3. - Surface of revolution with coordinates and velocity components.

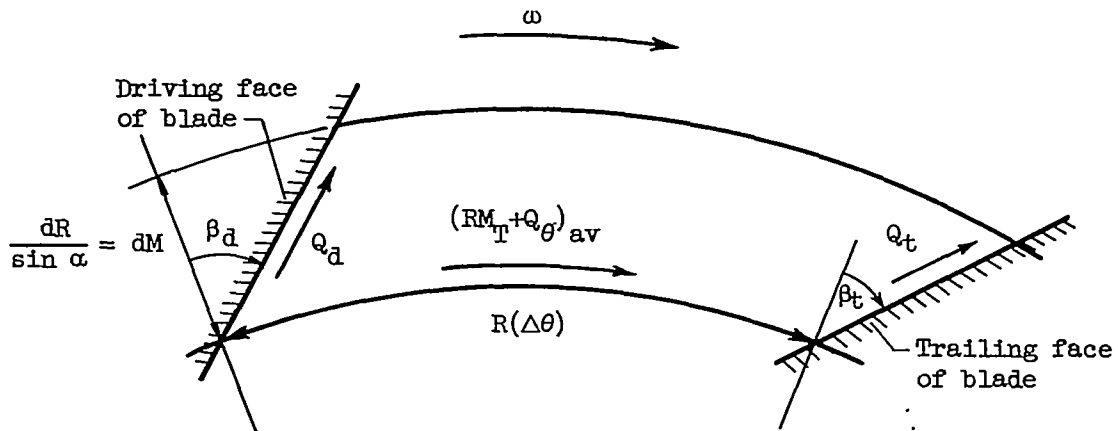


Figure 4. - Developed view of fluid strip between blades on surface of revolution at radius R.

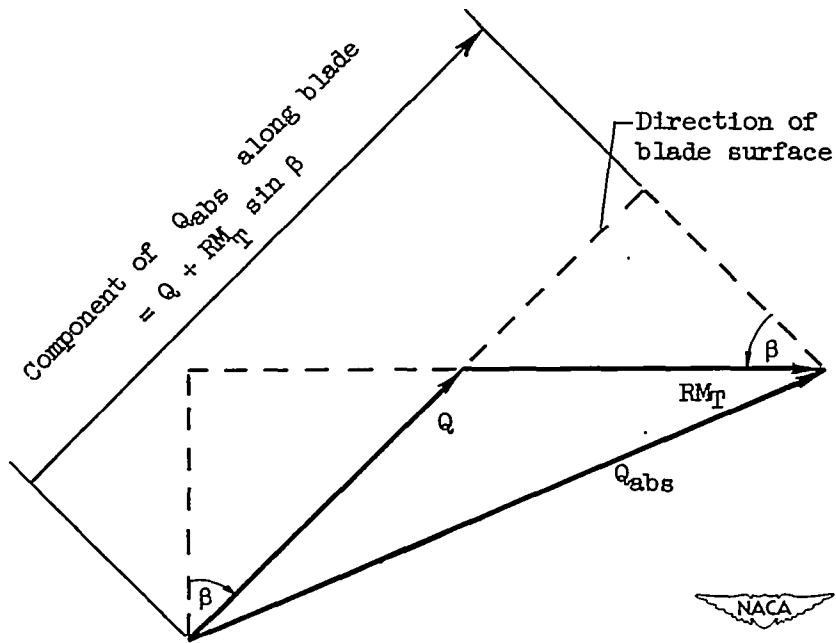


Figure 5. - Velocity triangle for computing component of absolute velocity along blade surface.

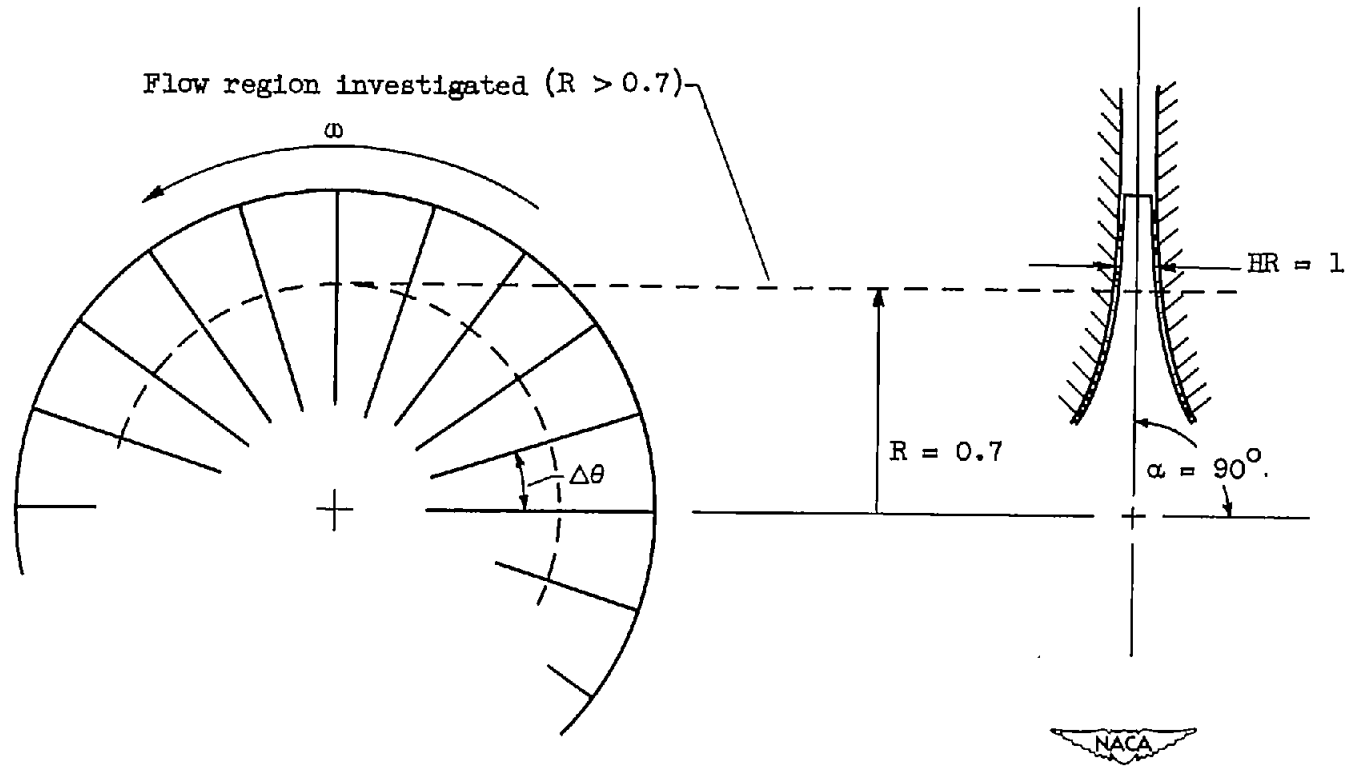
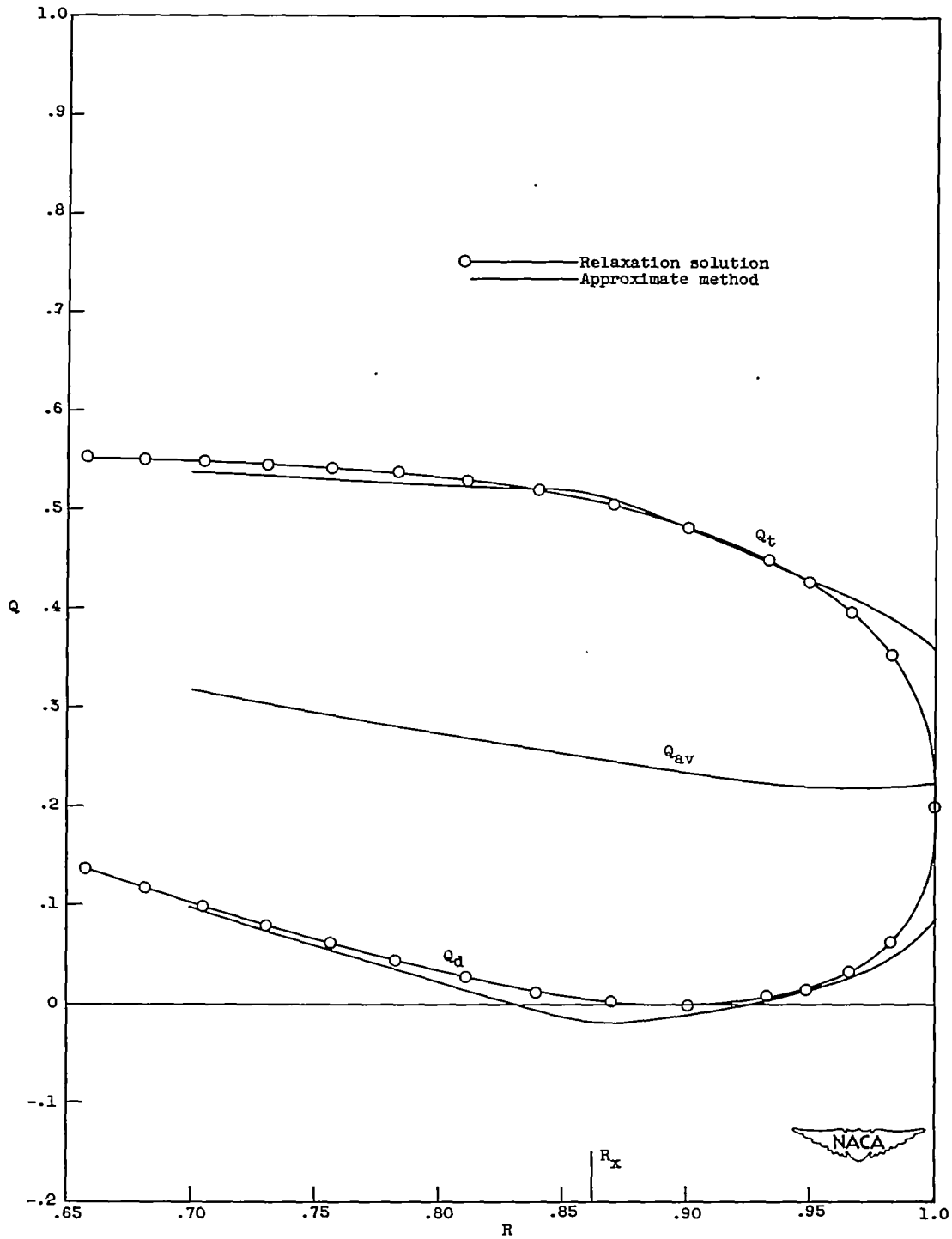


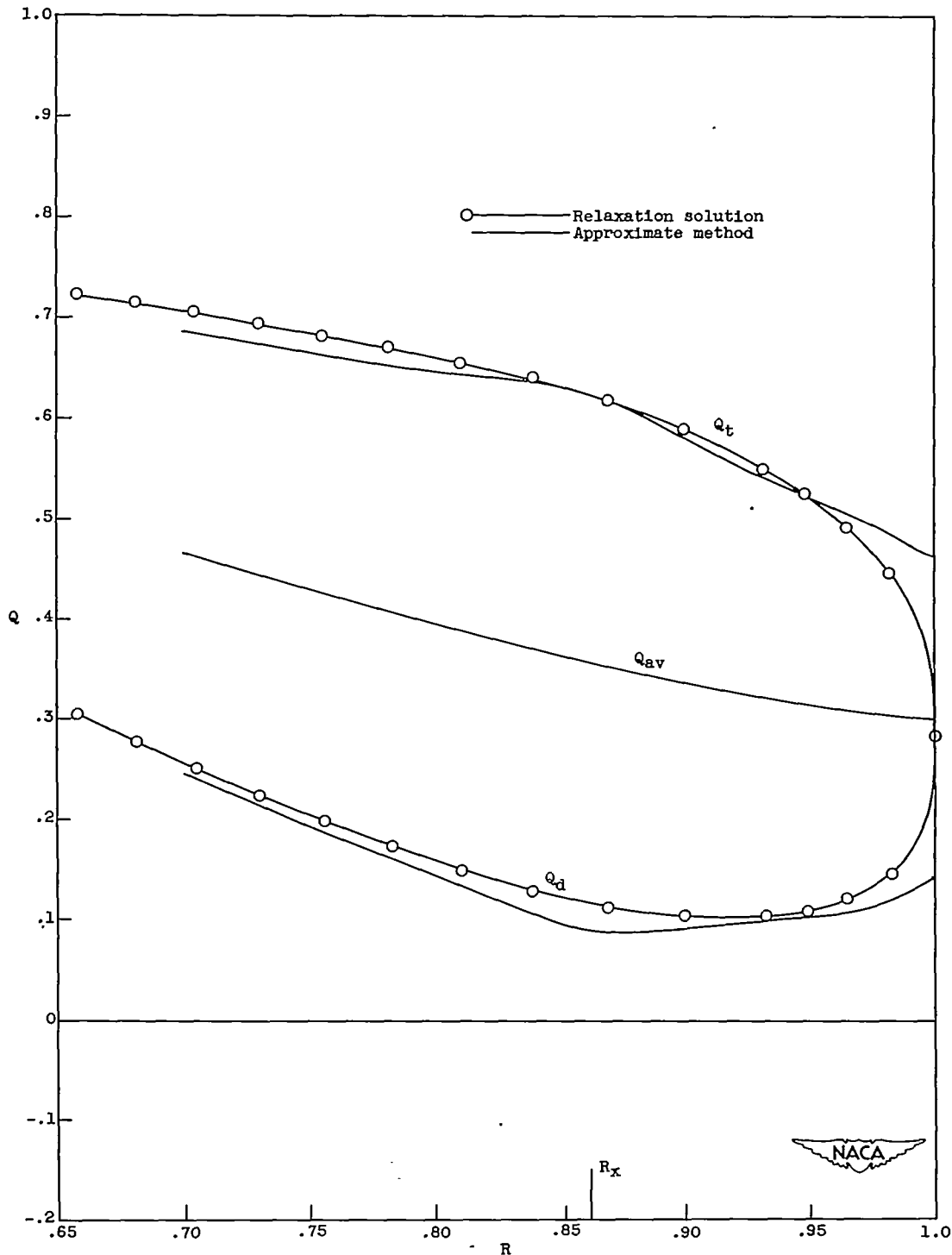
Figure 6. - Impeller-design characteristics for numerical examples.  
Straight impeller blades shown.





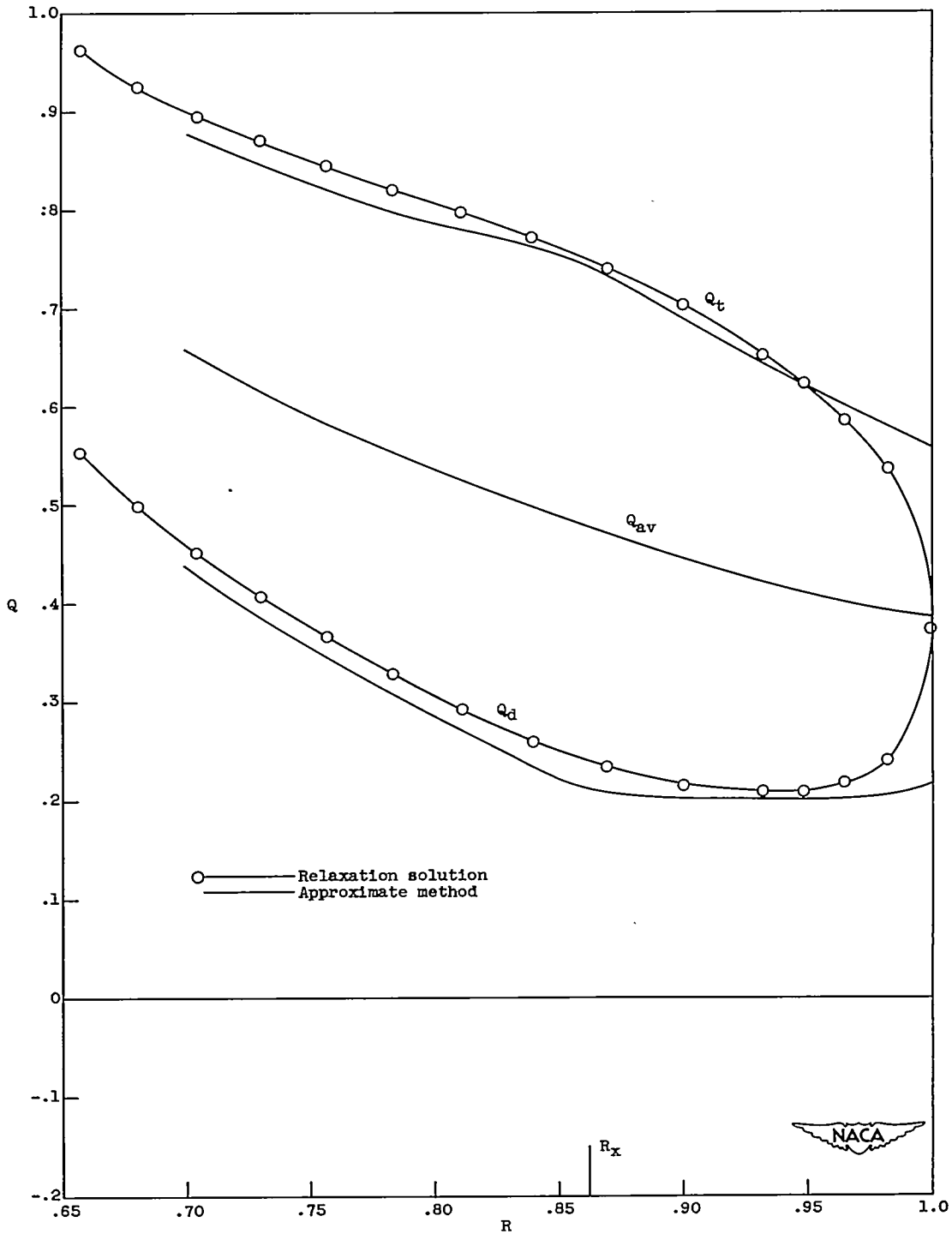
(a) Example (a): flow coefficient  $\phi$ , 0.5; impeller-tip Mach number  $M_{T_1}$ , 1.5; constant flow area ( $HR = 1.0$ ); angular width of passage  $\Delta\theta$ ,  $12^\circ$ ; blade angle  $\beta$ , 0; compressible flow ( $\gamma = 1.4$ ).

Figure 7. - Variation in velocity along blade surfaces as obtained by relaxation methods (references 1 and 7) and by approximate method.



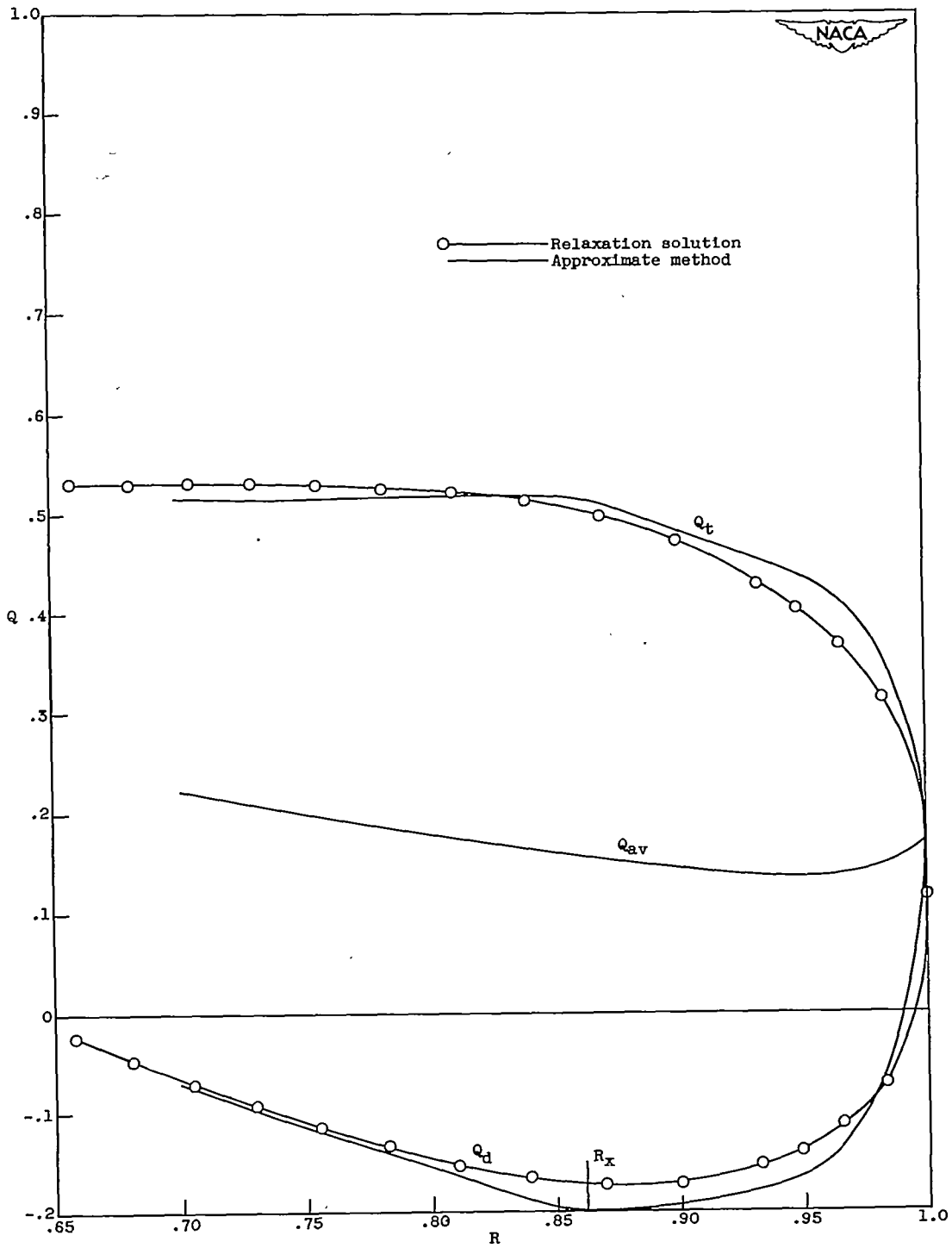
(b) Example (b): flow coefficient  $\phi$ , 0.7; other parameters same as example (a).

Figure 7. - Continued. Variation in velocity along blade surfaces as obtained by relaxation methods (references 1 and 7) and by approximate method.



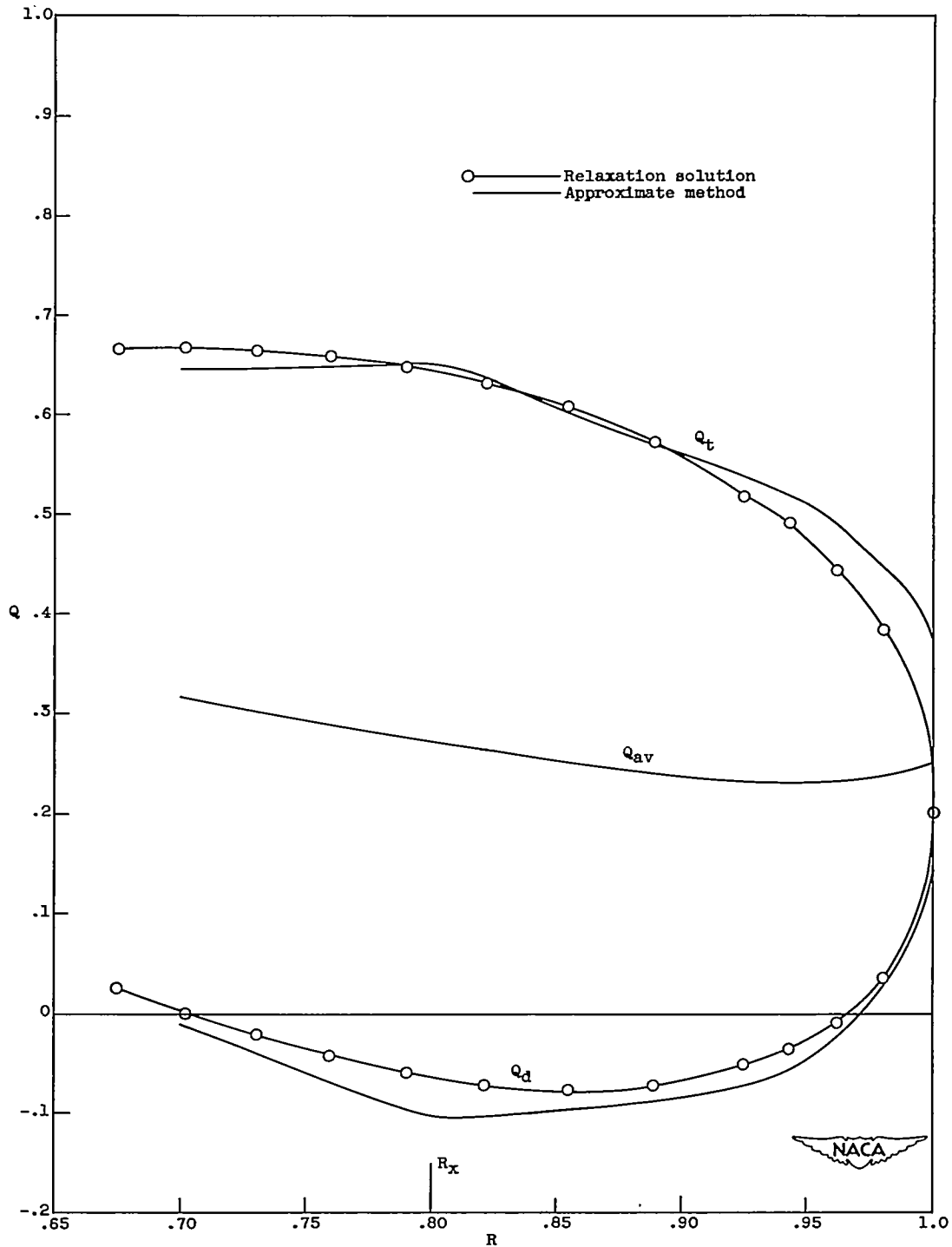
(c) Example (c): flow coefficient  $\phi$ , 0.9; other parameters same as example (a).

Figure 7. - Continued. Variation in velocity along blade surfaces as obtained by relaxation methods (references 1 and 7) and by approximate method.



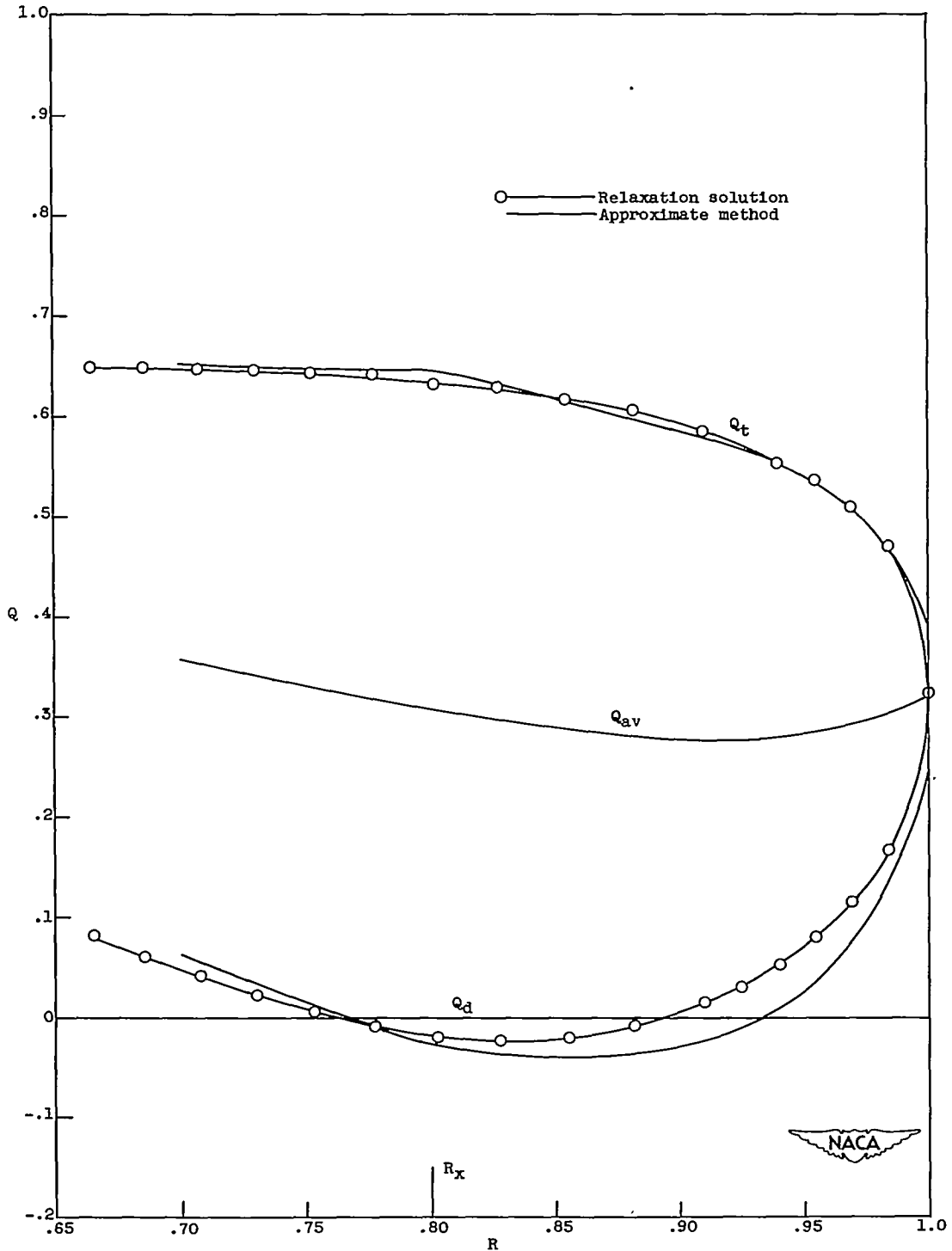
(d) Example (d): impeller-tip Mach number  $M_T$ , 2.0; other parameters same as example (a).

Figure 7. - Continued. Variation in velocity along blade surfaces as obtained by relaxation methods (references 1 and 7) and by approximate method.

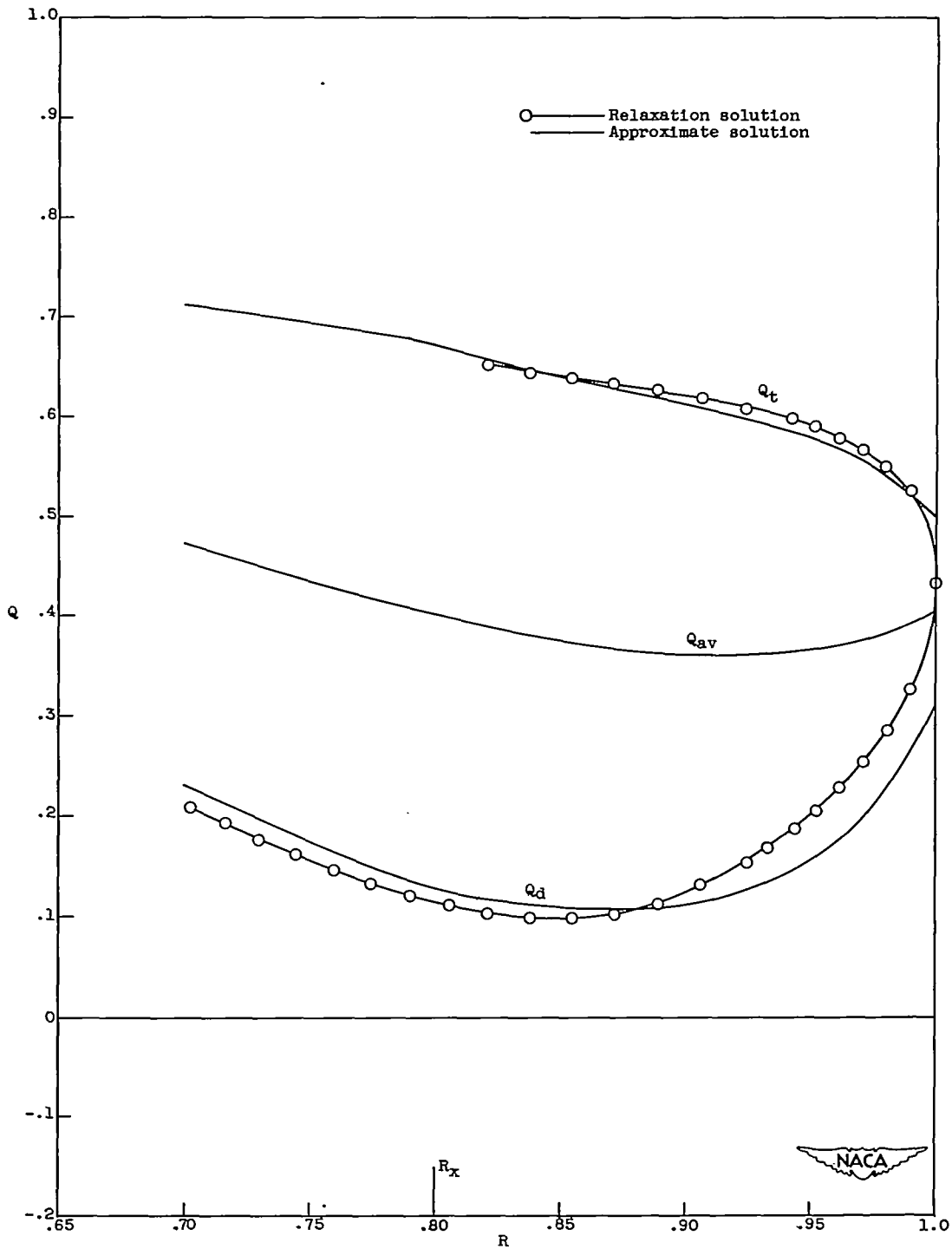


(e) Example (e): angular width of passage  $\Delta\theta$ ,  $18^\circ$ ; other parameters same as example (a).

Figure 7. - Continued. Variation in velocity along blade surfaces as obtained by relaxation methods (references 1 and 7) and by approximate method.

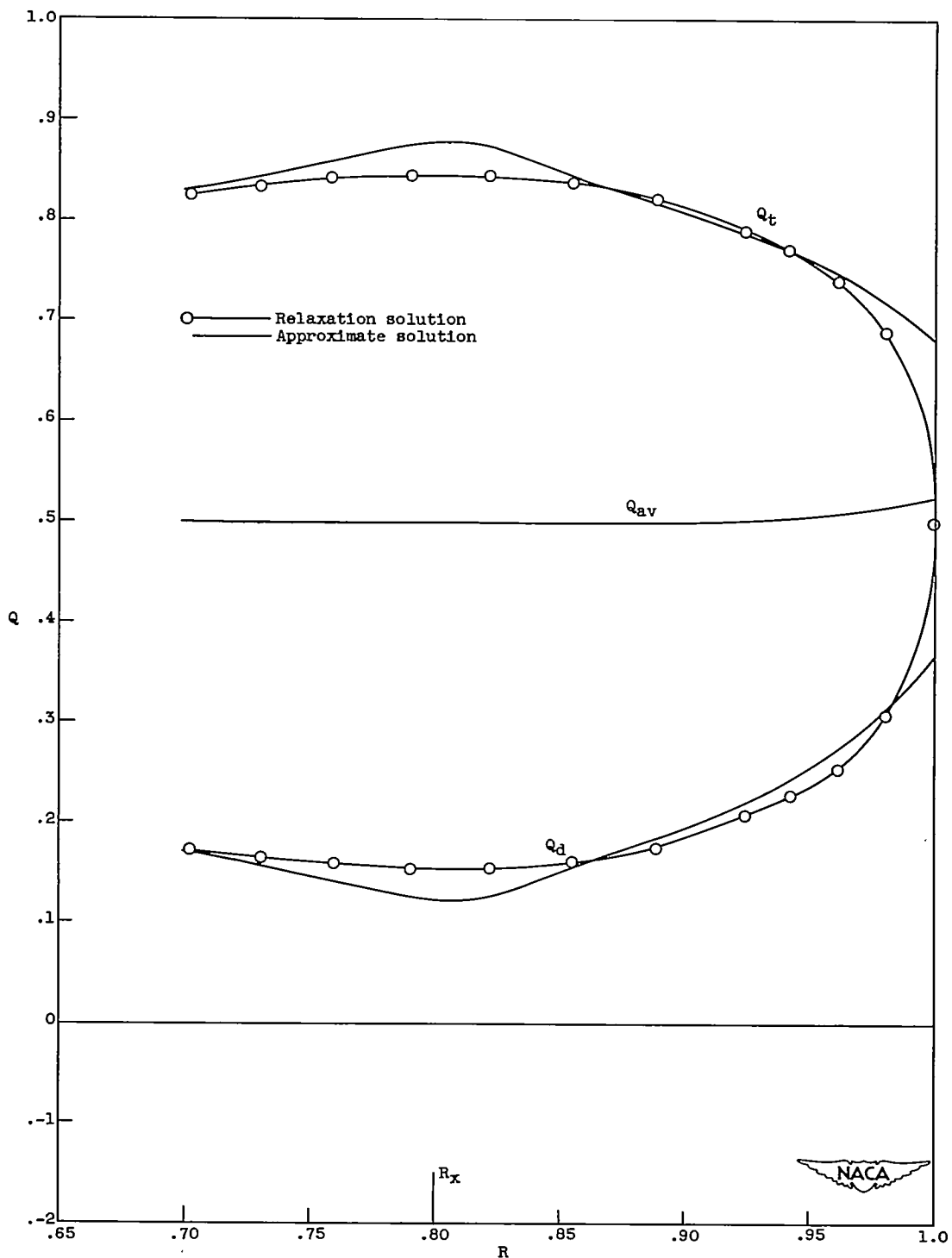


(f) Example (f): blade angle  $\beta$ ,  $\tan^{-1}(-0.5)$ ; other parameters same as example (e).  
 Figure 7. - Continued. Variation in velocity along blade surfaces as obtained by relaxation methods (references 1 and 7) and by approximate method.



(g) Example (g): blade angle  $\beta$ ,  $\tan^{-1}(-1.0)$ ; other parameters same as example (e).

Figure 7. - Continued. Variation in velocity along blade surfaces as obtained by relaxation methods (references 1 and 7) and by approximate method.



(h) Example (h): incompressible flow; other parameters same as example (e). Note that for incompressible flow stagnation speed of sound  $c_0$  contained in definitions of  $Q$ ,  $M_T$ , and  $\varphi$  is a fictitious quantity which, if considered equal to  $c_0$  of example (e), enables comparison of compressible (example (e)) and incompressible (example(h)) solutions for same impeller-tip speed, weight-flow rate, and so forth.

Figure 7. - Concluded. Variation in velocity along blade surfaces as obtained by relaxation methods (references 1 and 7) and by approximate method.